Physics Letters B 761 (2016) 179–183

Contents lists available at ScienceDirect

Physics Letters B

www.elsevier.com/locate/physletb

$W^{\pm}Z$ production at hadron colliders in NNLO QCD

Massimiliano Grazzini [a,*], Stefan Kallweit [b,c], Dirk Rathlev [d], Marius Wiesemann [a]

[a] Physik-Institut, Universität Zürich, CH-8057 Zürich, Switzerland
[b] PRISMA Cluster of Excellence, Institute of Physics, Johannes Gutenberg University, D-55099 Mainz, Germany
[c] Kavli Institute for Theoretical Physics, University of California, Santa Barbara, CA 93106, USA
[d] Theory Group, Deutsches Elektronen-Synchrotron, D-22607 Hamburg, Germany

ARTICLE INFO

Article history:
Received 6 May 2016
Received in revised form 9 July 2016
Accepted 8 August 2016
Available online 12 August 2016
Editor: G.F. Giudice

ABSTRACT

We report on the first computation of the next-to-next-to-leading order (NNLO) QCD corrections to $W^{\pm}Z$ production in proton collisions. We consider both the inclusive production of on-shell $W^{\pm}Z$ pairs at LHC energies and the total $W^{\pm}Z$ rates including off-shell effects of the W and Z bosons. In the off-shell computation, the invariant mass of the lepton pairs from the Z boson decay is required to be in a given mass window, and the results are compared with the corresponding measurements obtained by the ATLAS and CMS collaborations. The NNLO corrections range from 8% at $\sqrt{s} = 7$ TeV to 11% at $\sqrt{s} = 14$ TeV and significantly improve the agreement with the LHC data at $\sqrt{s} = 7$ and 8 TeV.

The production of $W^{\pm}Z$ pairs at the Large Hadron Collider (LHC) provides an important test of the electroweak (EW) sector of the Standard Model (SM) at the TeV scale. Due to its sensitivity to the gauge-boson self-interactions, small deviations in the observed rates or in the kinematical distributions could give a hint of new physics. Such effects can be modelled on the basis of higher-dimensional operators in the form of anomalous couplings. With the increasing reach in energy of LHC Run 2, $W^{\pm}Z$ measurements will be a powerful tool to extend the current bounds on these effective couplings. The $W^{\pm}Z$ process also constitutes an irreducible background in many new-physics searches, see for example Ref. [1].

With its relatively small cross section $W^{\pm}Z$ production yielded only a limited number of events at the Tevatron [2,3], but its cross section has been measured with good precision at the LHC by both ATLAS [4,5] and CMS [6] at centre-of-mass energies of 7 and 8 TeV. An early measurement of the $W^{\pm}Z$ cross section at 13 TeV by CMS is also already available [7].

On the theory side, the first next-to-leading order (NLO) predictions for on-shell $W^{\pm}Z$ production were obtained long ago [8]. Leptonic decays were added in Ref. [9], initially neglecting spin correlations in the virtual matrix elements. The computation of the relevant one-loop helicity amplitudes [10] enabled the first complete NLO calculations [11–13], including spin correlations and off-shell effects. The NLO QCD corrections to off-shell $W^{\pm}Z + \text{jet}$ production were presented in Ref. [14], and the on-shell EW corrections to $W^{\pm}Z$ production in Refs. [15,16].

While the W^+W^- and ZZ cross sections can be computed at NNLO in the on-shell approximation using two-loop amplitudes for two massive vector bosons of the same mass, as done in Ref. [17] and Ref. [18], respectively, the $W^{\pm}Z$ production process requires the amplitudes with different masses of the vector-boson pairs already in the on-shell approximation. The required two-loop amplitudes were presented in Refs. [19,20] in the form of helicity amplitudes for all vector-boson pair production processes, enabling at the same time the computation of NNLO corrections to $W^{\pm}Z$ production as well as the inclusion of off-shell effects and the leptonic decays of the vector bosons at the NNLO level. In the meantime, the implementation of the two-loop form factors for the helicity amplitudes into a numerical code provided by the authors of Ref. [20] has been used to obtain NNLO predictions for the $ZZ \to 4\ell$ process in Ref. [21] and the $W^+W^- \to 2\ell 2\nu$ process in Ref. [22].

$W^{\pm}Z$ production is the only remaining diboson process for which a complete NNLO calculation was not available so far. In this letter, we finally close this gap by providing NNLO predictions for the $W^{\pm}Z$ cross section at various LHC energies, which thus represents an important milestone in the NNLO programme. We restrict ourselves to presenting inclusive results, both for on-shell $W^{\pm}Z$ production, and including all off-shell effects, but applying minimal mass cuts on the reconstructed Z boson. Our off-shell calculation in particular includes the singly-resonant contributions of the form $pp \to W^{\pm} \to 3\ell\nu$, the resonant $W^{\pm}\gamma^*$ contributions and all interference terms. The computation presented here thus

* Corresponding author.
E-mail address: grazzini@physik.uzh.ch (M. Grazzini).

http://dx.doi.org/10.1016/j.physletb.2016.08.017

Table 1
Total on-shell $W^{\pm}Z$ cross sections at LO, NLO and NNLO for relevant collider energies; the last two columns contain the relative corrections at NLO and NNLO, respectively.

$\sqrt{s}$ [TeV]	$\sigma_{\rm LO}$ [pb]	$\sigma_{\rm NLO}$ [pb]	$\sigma_{\rm NNLO}$ [pb]	$\sigma_{\rm NLO}/\sigma_{\rm LO}$	$\sigma_{\rm NNLO}/\sigma_{\rm NLO}$
7	$11.354(1)\,^{+0.5\%}_{-1.2\%}$	$18.500(1)\,^{+5.3\%}_{-4.1\%}$	$19.973(13)\,^{+1.7\%}_{-1.9\%}$	+62.9%	+8.0%
8	$13.654(1)\,^{+1.3\%}_{-2.1\%}$	$22.750(2)\,^{+5.1\%}_{-3.9\%}$	$24.690(16)\,^{+1.8\%}_{-1.9\%}$	+66.6%	+8.5%
13	$25.517(2)\,^{+4.3\%}_{-5.3\%}$	$46.068(3)\,^{+4.9\%}_{-3.9\%}$	$51.11(3)\,^{+2.2\%}_{-2.0\%}$	+80.5%	+10.9%
14	$27.933(2)\,^{+4.7\%}_{-5.7\%}$	$51.038(3)\,^{+5.0\%}_{-4.0\%}$	$56.85(3)\,^{+2.3\%}_{-2.0\%}$	+82.7%	+11.4%

paves the way to a fully-differential computation of the process $pp \to \ell^{(\prime)\pm}\nu_{\ell^{(\prime)}}\ell^+\ell^-$ in the future.

Our calculation is performed with the numerical program MATRIX[1], which combines the q_T-subtraction [23] and -resummation [24] formalisms with the MUNICH Monte-Carlo framework.[2] MUNICH provides a fully-automated implementation of the Catani–Seymour dipole subtraction method [25,26], an efficient phase-space integration, as well as an interface to the one-loop generator OPENLOOPS [27] to obtain all required (spin- and colour-correlated) tree-level and one-loop amplitudes. For the numerically stable evaluation of tensor integrals, OPENLOOPS relies on the COLLIER library [28,29], which is based on the Denner–Dittmaier reduction techniques [30,31] and the scalar integrals of Ref. [32]. To deal with problematic phase-space points, a rescue system is provided, which employs the quadruple-precision implementation of the OPP method in CUTTOOLS [33] and scalar integrals from ONELOOP [34]. Our implementation of q_T subtraction and resummation[3] for the production of colourless final states is fully general, and it is based on the universality of the hard-collinear coefficients [37] appearing in the transverse-momentum resummation formalism. These coefficients were explicitly computed for quark-initiated processes in Refs. [38–40]. For the two-loop helicity amplitudes we use the results of Ref. [20], and of Ref. [41] for Drell–Yan like topologies.

A preliminary version of MATRIX has been employed in the NNLO computations of Refs. [17,18,21,22,42,43], and in the resummed calculation of Ref. [35].

We consider proton–proton collisions with $\sqrt{s} = 7, 8, 13$ and 14 TeV. As far as EW couplings are concerned, we use the so-called G_μ scheme, where the input parameters are G_F, m_W, m_Z. More precisely and consistent with the OPENLOOPS implementation, we use the complex W and Z boson masses to define the EW mixing angle as $\cos\theta_W^2 = (m_W^2 - i\Gamma_W m_W)/(m_Z^2 - i\Gamma_Z m_Z)$, and set $G_F = 1.16639 \times 10^{-5}\,\text{GeV}^{-2}$, $m_W = 80.385\,\text{GeV}$, $\Gamma_W = 2.0854\,\text{GeV}$, $m_Z = 91.1876\,\text{GeV}$, $\Gamma_Z = 2.4952\,\text{GeV}$. With these inputs, the relevant leading-order branching fractions are $BR(W^\pm \to \nu\ell^\pm) = 0.108984$ and $BR(Z \to \ell^+\ell^-) = 0.0336313$. We set the CKM matrix to unity[4]. We employ the NNPDF3.0 [44] sets of parton distributions with $\alpha_S(m_Z) = 0.118$. Predictions at N^{n}LO (with $n = 0, 1, 2$) are obtained by using PDFs at the corresponding perturbative order and the evolution of α_S at $(n+1)$-loop order, as provided by the PDF set. We consider $N_f = 5$ massless quark flavours. The central renormalisation (μ_R) and factorisation (μ_F) scales are set to $\mu_R = \mu_F = \mu_0 \equiv \frac{1}{2}(m_Z + m_W) = 85.7863\,\text{GeV}$. Scale uncertainties

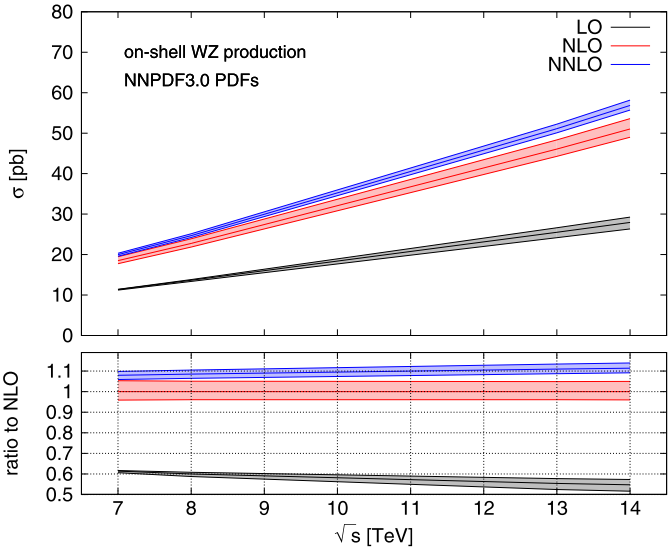

Fig. 1. On-shell $W^{\pm}Z$ cross section as a function of the centre-of-mass energy at LO, NLO and NNLO. In the lower panel the curves of the main frame are normalised to the central NLO prediction. The bands correspond to scale variations as described in the text.

are computed by the customary 7-point variation, i.e., we vary independently $0.5\mu_0 \le \mu_R, \mu_F \le 2\mu_0$ with the constraint $0.5 \le \mu_R/\mu_F \le 2$. If not stated otherwise, all cross sections presented in the following are summed over the electrical charges of the final-state W bosons, i.e. they refer to $\sigma(pp \to W^+Z) + \sigma(pp \to W^-Z)$.

We start the presentation of our results by considering the on-shell $W^{\pm}Z$ cross sections[5]. In Table 1 we report the LO, NLO and NNLO cross sections and scale uncertainties in the $\sqrt{s}$ range from 7 to 14 TeV. The same results are shown in Fig. 1. The main interest of these on-shell results is that they can be unambiguously defined without choosing a specific mass window for the Z boson decay products. Consistent with Ref. [13], the NLO corrections are quite large and increase the LO result by 63% to 83% for centre-of-mass energies between 7 and 14 TeV. The NNLO corrections further increase the NLO results, and the effect ranges from 8% to 11%. We note that in contrast to ZZ and W^+W^- production, these are purely genuine NNLO corrections to the $q\bar{q}$ channel: As the Born-level final state is electrically charged, the production process does not receive contributions from a loop-induced gluon–fusion channel. Due to the absence of such a loop-induced gluon–gluon channel, which usually features large corrections, NLO scale variations might be expected to give a reliable estimate of possible effects at the NNLO and beyond. However, this turns out to be not the case in general: In particular at large collider energies, the NNLO corrections are roughly twice as large as the uncertainties

[1] MATRIX is the abbreviation of "MUNICH Automates qT subtraction and Resummation to Integrate Cross Sections", by M. Grazzini, S. Kallweit, D. Rathlev, M. Wiesemann. In preparation.

[2] S. Kallweit, Munich is the abbreviation of "MUlti-chaNnel Integrator at Swiss (CH) precision"—an automated parton level NLO generator, 2016, in preparation.

[3] The first application of the transverse-momentum resummation framework implemented in MATRIX at NNLL+NNLO to on-shell W^+W^- and ZZ production was presented in Ref. [35] (see also Ref. [36] for more details).

[4] The numerical effect of the CKM matrix up to NLO is to reduce the cross section by less than 1%.

[5] In this on-shell computation, the gauge-boson widths are set to zero, and a real EW mixing angle is used correspondingly.

Table 2
Total on-shell $W^{\pm}Z$ cross sections at LO, NLO and NNLO, together with the relative corrections to the respective lower order, for relevant collider energies, separated according to the charge of the final states.

$\sqrt{s}$ [TeV]	Process	$\sigma_{\rm LO}$ [pb]	$\sigma_{\rm NLO}$ [pb]	$\sigma_{\rm NNLO}$ [pb]	$\sigma_{\rm NLO}/\sigma_{\rm LO}$	$\sigma_{\rm NNLO}/\sigma_{\rm NLO}$
7	W^+Z	$7.343(1)^{+0.4\%}_{-1.1\%}$	$11.867(1)^{+5.3\%}_{-4.1\%}$	$12.790(11)^{+1.8\%}_{-1.9\%}$	+61.6%	+7.8%
	W^-Z	$4.011(1)^{+0.7\%}_{-1.4\%}$	$6.633(1)^{+5.4\%}_{-4.1\%}$	$7.183(6)^{+1.7\%}_{-1.9\%}$	+65.4%	+8.3%
8	W^+Z	$8.741(1)^{+1.2\%}_{-2.0\%}$	$14.443(1)^{+5.0\%}_{-3.9\%}$	$15.650(14)^{+1.9\%}_{-1.9\%}$	+65.2%	+8.4%
	W^-Z	$4.913(1)^{+1.5\%}_{-2.3\%}$	$8.307(1)^{+5.1\%}_{-3.9\%}$	$9.040(8)^{+1.8\%}_{-1.8\%}$	+69.1%	+8.8%
13	W^+Z	$15.787(2)^{+4.1\%}_{-5.1\%}$	$28.251(3)^{+4.9\%}_{-3.9\%}$	$31.33(3)^{+2.3\%}_{-2.0\%}$	+79.0%	+10.9%
	W^-Z	$9.730(1)^{+4.5\%}_{-5.5\%}$	$17.817(2)^{+4.9\%}_{-4.0\%}$	$19.78(2)^{+2.2\%}_{-2.0\%}$	+83.1%	+11.0%
14	W^+Z	$17.199(2)^{+4.6\%}_{-5.6\%}$	$31.147(3)^{+4.9\%}_{-4.0\%}$	$34.68(3)^{+2.4\%}_{-2.1\%}$	+81.1%	+11.3%
	W^-Z	$10.733(1)^{+4.9\%}_{-6.0\%}$	$19.891(2)^{+5.0\%}_{-4.0\%}$	$22.17(2)^{+2.2\%}_{-2.0\%}$	+85.3%	+11.4%

Table 3
Total cross sections with ATLAS mass window $66\,{\rm GeV} < m(Z) < 116\,{\rm GeV}$ at LO, NLO and NNLO. The available ATLAS data from Refs. [4,5] are also shown.

$\sqrt{s}$ [TeV]	$\sigma_{\rm LO}$ [pb]	$\sigma_{\rm NLO}$ [pb]	$\sigma_{\rm NNLO}$ [pb]	$\sigma_{\rm ATLAS}$ [pb]
7	$11.028(8)^{+0.5\%}_{-1.2\%}$	$17.93(1)^{+5.3\%}_{-4.1\%}$	$19.34(3)^{+1.6\%}_{-1.8\%}$	$19.0\,^{+1.4}_{-1.3}({\rm stat})^{+0.9}_{-0.9}({\rm syst})^{+0.4}_{-0.4}({\rm lumi})$
8	$13.261(9)^{+1.3\%}_{-2.1\%}$	$22.03(2)^{+5.1\%}_{-3.9\%}$	$23.92(3)^{+1.7\%}_{-1.8\%}$	$24.3\,^{+0.6}_{-0.6}({\rm stat})^{+0.6}_{-0.6}({\rm syst})^{+0.5}_{-0.5}({\rm lumi})^{+0.4}_{-0.4}({\rm th})$
13	$24.79(2)^{+4.2\%}_{-5.2\%}$	$44.67(3)^{+4.9\%}_{-3.9\%}$	$49.62(6)^{+2.2\%}_{-2.0\%}$	
14	$27.14(2)^{+4.7\%}_{-5.7\%}$	$49.50(3)^{+4.9\%}_{-4.0\%}$	$55.10(7)^{+2.3\%}_{-2.0\%}$	

estimated by scale variations at NLO. We note that the scale uncertainties drop from about $\pm 5\%$ at NLO to about $\pm 2\%$ at NNLO.

Similarly to what happens in the case of $W\gamma$ production [43], the rather large impact of radiative corrections is due to the existence of a *radiation zero* in the Born scattering amplitudes. More precisely, the partonic $W\gamma$ tree amplitude exhibits an *exact* radiation zero at $\theta^* = 1/3$, where θ^* is the scattering angle in the centre-of-mass frame [45]. Analogously, the partonic on-shell Born $W^{\pm}Z$ amplitude exhibits an *approximate* radiation zero [46][6]. The radiation zero is broken by real corrections starting from the NLO, but suppresses the LO cross section, thus leading to an increased impact of higher-order corrections.

For completeness, in Table 2 we provide cross sections and relative corrections for the two contributing processes $pp \to W^+Z$ and $pp \to W^-Z$. The W^+Z rate, being driven by $u\bar{d}$ scattering, is larger than the W^-Z rate, which is driven by $d\bar{u}$ scattering. The difference decreases as $\sqrt{s}$ increases. As expected, radiative corrections to the two processes are very similar. They turn out to be slightly larger for W^-Z than for W^+Z, leading to a reduction of the $\sigma^{W^+Z}/\sigma^{W^-Z}$ ratio at higher perturbative orders. This difference in the ratios, however, is due to differences in the PDFs used at each order, and it decreases with increasing collider energies, never exceeding 1% at the NNLO.

From now on, all our results contain the full off-shell effects. The ATLAS and CMS collaborations report inclusive $W^{\pm}Z$ cross sections obtained by considering a mass window on the reconstructed Z boson. The mass window slightly differs between ATLAS and CMS: While ATLAS uses $66\,{\rm GeV} < m(Z) < 116\,{\rm GeV}$ for their measurements at 7 and 8 TeV (a measurement at 13 TeV has not been published so far), CMS applies a cut of $71\,{\rm GeV} < m(Z) < 111\,{\rm GeV}$ for their measurements at 7 and 8 TeV and $60\,{\rm GeV} < m(Z) < 120\,{\rm GeV}$ for their measurement at 13 TeV. We find that the numerical differences between the cross sections computed in the different mass windows are at the 1% level, and thus significantly smaller than the current experimental uncertainties. When considering the relative effects of radiative corrections, the impact of the different mass windows is completely negligible. Nevertheless, we will consistently apply the respective mass windows when comparing to data in the following.

We first present results for the ATLAS definition of the $W^{\pm}Z$ cross sections, reported in Table 3, where we compare with the 7 and 8 TeV ATLAS measurements of Ref. [4] and Ref. [5], respectively. Comparing these cross sections in absolute terms to the on-shell case, we find a reduction by roughly 3% due to the applied mass-window cut and genuine off-shell effects; however, as anticipated, the relative impact of radiative corrections remains widely unchanged, again ranging between 63% and 83% at NLO and between 8% and 11% at NNLO for the collider energies under consideration. Also the scale uncertainty bands stay almost identical when including off-shell effects and applying the ATLAS mass cut.

Comparing with the experimentally measured cross sections from Refs. [4,5], we find that the inclusion of NNLO corrections clearly improves the agreement between data and theory, in particular at 8 TeV, where the measurement is most precise. While the central NLO prediction is roughly 2σ away from the measured cross section at 8 TeV, the NNLO prediction is right on top of the data with fully overlapping uncertainty bands.

[6] The approximate nature of the radiation zero for $W^{\pm}Z$ production is due to the fact that it appears only in the dominant helicity amplitudes for this process [46]. On the contrary, the $W\gamma$ process has an exact zero in all the helicity amplitudes, due to the presence of the massless photon.

Table 4
Total cross sections with CMS mass windows of 71 GeV $< m(Z) <$ 111 GeV for 7 and 8 TeV, and 60 GeV $< m(Z) <$ 120 GeV for 13 and 14 TeV, at LO, NLO and NNLO. The available CMS data from Refs. [6,7] are also shown.

$\sqrt{s}$ [TeV]	$\sigma_{\rm LO}$ [pb]	$\sigma_{\rm NLO}$ [pb]	$\sigma_{\rm NNLO}$ [pb]	$\sigma_{\rm CMS}$ [pb]
7	$10.902(7)^{+0.5\%}_{-1.2\%}$	$17.72(1)^{+5.3\%}_{-4.1\%}$	$19.18(3)^{+1.7\%}_{-1.8\%}$	$20.76^{+1.32}_{-1.32}(\text{stat})^{+1.13}_{-1.13}(\text{syst})^{+0.46}_{-0.46}(\text{lumi})$
8	$13.115(9)^{+1.3\%}_{-2.1\%}$	$21.80(2)^{+5.1\%}_{-3.9\%}$	$23.68(3)^{+1.8\%}_{-1.8\%}$	$24.61^{+0.76}_{-0.76}(\text{stat})^{+1.13}_{-1.13}(\text{syst})^{+1.08}_{-1.08}(\text{lumi})$
13	$25.04(2)^{+4.3\%}_{-5.3\%}$	$45.09(3)^{+4.9\%}_{-3.9\%}$	$49.98(6)^{+2.2\%}_{-2.0\%}$	$40.9^{+3.4}_{-3.4}(\text{stat})^{+3.1}_{-3.3}(\text{syst})^{+1.3}_{-1.3}(\text{lumi})^{+0.4}_{-0.4}(\text{th})$
14	$27.39(2)^{+4.7\%}_{-5.7\%}$	$49.91(4)^{+4.9\%}_{-4.0\%}$	$55.60(7)^{+2.3\%}_{-2.0\%}$	

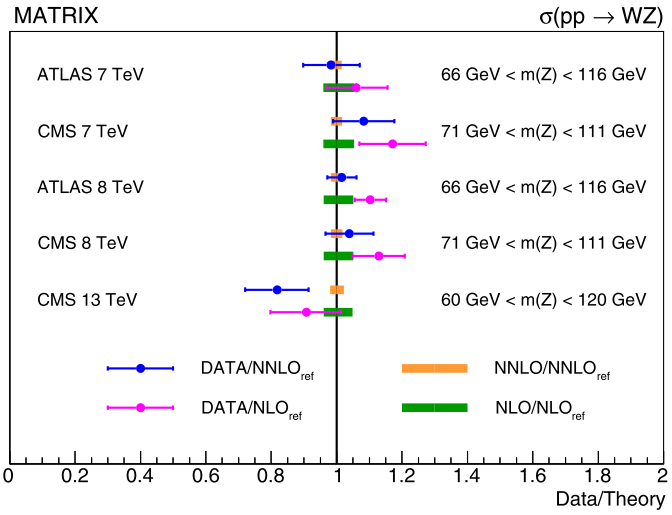

Fig. 2. Summary plot for comparison of NLO and NNLO predictions with the available LHC measurements of the total $W^{\pm}Z$ cross section. Theory uncertainties are obtained through scale variations as described in the text.

Next, we provide theory predictions for the $W^{\pm}Z$ cross sections as defined by CMS in Table 4, where we also quote the results of the CMS measurements performed at 7 and 8 TeV (reported in Ref. [6]), and at 13 TeV (reported in Ref. [7]). As already anticipated, the precise definition of the Z-mass window has only a very mild impact on the cross section. In particular, both the relative size of higher-order corrections and the bands obtained by scale variation are almost identical to the ones obtained with the ATLAS definition. Comparing with the measured cross sections, we again find excellent agreement between our NNLO predictions and the cross sections reported by CMS for $\sqrt{s} = 7$ and 8 TeV, where the inclusion of NNLO corrections again clearly improves the agreement, in particular at 8 TeV. The measurement at 13 TeV undershoots the NNLO prediction, being consistent with it only at the level of about 2σ. However, at this early stage of LHC Run 2, the measurement still comes with quite large experimental uncertainties of both systematical and statistical nature, and the measured cross section might still be subject to a significant shift with respect to its central value, once statistics increases.

Fig. 2 shows a summary plot where we compare NLO and NNLO predictions to all available LHC measurements of the total $W^{\pm}Z$ cross section.

We have presented the first exact NNLO QCD computation for the production of $W^{\pm}Z$ pairs at the LHC. We have considered both the case in which the vector bosons are on shell, and the case in which off-shell effects are accounted for. The NNLO corrections are sizeable and range from about 8% at $\sqrt{s} = 7$ TeV to about 11% at $\sqrt{s} = 14$ TeV with respect to the NLO prediction, significantly exceeding what might be expected from NLO scale variations. The remaining scale uncertainties at NNLO are at the level of about 2%. We have stressed that the large size of QCD radiative corrections is due to an approximate radiation zero which is present in the on-shell amplitude at LO. Nonetheless, since all partonic channels are included at NNLO, and the NNLO corrections, although significant, are still much smaller than the NLO effects, we expect that scale variations should provide the correct order of magnitude of the uncertainty from yet uncalculated higher-order QCD corrections beyond NNLO. EW corrections would affect our results at the 1% level or less [15,16]. PDF uncertainties are expected to be at the 1–2% level.

When off-shell effects for the W and Z bosons are accounted for, our results can be compared to the inclusive cross sections presented by ATLAS and CMS, provided the same range in the virtuality of the Z boson is imposed. We find that the inclusion of NNLO corrections is mandatory in order to obtain agreement (within 1σ) with the inclusive cross sections measured by ATLAS and CMS in Run 1 of the LHC. The computed corrections will be even more important at 13 TeV, once enough statistics is accumulated. Since our computation already involves the full helicity amplitudes and all off-shell effects, it can be extended to include realistic selection cuts on the final-state leptons and to provide predictions in the fiducial volume in which the measurements are carried out. It will also be possible to provide precise background predictions in new-physics searches based on the trilepton + missing energy signature.

Our calculation was performed with the numerical program MATRIX, which is able to carry out fully-exclusive NNLO computations for a wide class of processes at hadron colliders. We are planning further applications of our framework to other important LHC processes.

Acknowledgements

This research was supported in part by the Swiss National Science Foundation (SNF) under contracts CRSII2-141847, 200021-156585, by the Research Executive Agency (REA) of the European Union under the Grant Agreement number PITN–GA–2012–316704 (*HiggsTools*), and by the National Science Foundation under Grant No. NSF PHY11-25915.

References

[1] D.E. Morrissey, T. Plehn, T.M.P. Tait, Phys. Rep. 515 (2012) 1, arXiv:0912.3259 [hep-ph].
[2] E.D. Lipeles, CDF Collaboration, Conf. Proc. C 060726 (2006) 689, arXiv:hep-ex/0701038.
[3] V.M. Abazov, et al., D0 Collaboration, Phys. Rev. D 85 (2012) 112005, arXiv:1201.5652 [hep-ex].
[4] G. Aad, et al., ATLAS Collaboration, Eur. Phys. J. C 72 (2012) 2173, arXiv:1208.1390 [hep-ex].
[5] G. Aad, et al., ATLAS Collaboration, arXiv:1603.02151 [hep-ex].
[6] CMS Collaboration, CMS-PAS-SMP-12-006.
[7] CMS Collaboration, CMS-PAS-SMP-16-002.

[8] J. Ohnemus, Phys. Rev. D 44 (1991) 3477.
[9] J. Ohnemus, Phys. Rev. D 50 (1994) 1931, arXiv:hep-ph/9403331.
[10] L.J. Dixon, Z. Kunszt, A. Signer, Nucl. Phys. B 531 (1998) 3, arXiv:hep-ph/9803250.
[11] L.J. Dixon, Z. Kunszt, A. Signer, Phys. Rev. D 60 (1999) 114037, arXiv:hep-ph/9907305.
[12] J.M. Campbell, R.K. Ellis, Phys. Rev. D 60 (1999) 113006, arXiv:hep-ph/9905386.
[13] J.M. Campbell, R.K. Ellis, C. Williams, J. High Energy Phys. 1107 (2011) 018, arXiv:1105.0020 [hep-ph].
[14] F. Campanario, C. Englert, S. Kallweit, M. Spannowsky, D. Zeppenfeld, J. High Energy Phys. 1007 (2010) 076, arXiv:1006.0390 [hep-ph].
[15] A. Bierweiler, T. Kasprzik, J.H. Kühn, J. High Energy Phys. 1312 (2013) 071, arXiv:1305.5402 [hep-ph].
[16] J. Baglio, L.D. Ninh, M.M. Weber, Phys. Rev. D 88 (2013) 113005, arXiv:1307.4331.
[17] F. Cascioli, T. Gehrmann, M. Grazzini, S. Kallweit, P. Maierhöfer, A. von Manteuffel, S. Pozzorini, D. Rathlev, L. Tancredi, E. Weihs, Phys. Lett. B 735 (2014) 311, arXiv:1405.2219 [hep-ph].
[18] T. Gehrmann, M. Grazzini, S. Kallweit, P. Maierhöfer, A. von Manteuffel, S. Pozzorini, D. Rathlev, L. Tancredi, Phys. Rev. Lett. 113 (21) (2014) 212001, arXiv:1408.5243 [hep-ph].
[19] F. Caola, J.M. Henn, K. Melnikov, A.V. Smirnov, V.A. Smirnov, J. High Energy Phys. 1411 (2014) 041, arXiv:1408.6409 [hep-ph].
[20] T. Gehrmann, A. von Manteuffel, L. Tancredi, arXiv:1503.04812 [hep-ph].
[21] M. Grazzini, S. Kallweit, D. Rathlev, Phys. Lett. B 750 (2015) 407, arXiv:1507.06257 [hep-ph].
[22] M. Grazzini, S. Kallweit, S. Pozzorini, D. Rathlev, M. Wiesemann, arXiv:1605.02716 [hep-ph].
[23] S. Catani, M. Grazzini, Phys. Rev. Lett. 98 (2007) 222002, arXiv:hep-ph/0703012.
[24] G. Bozzi, S. Catani, D. de Florian, M. Grazzini, Nucl. Phys. B 737 (2006) 73, arXiv:hep-ph/0508068.
[25] S. Catani, M.H. Seymour, Phys. Lett. B 378 (1996) 287, arXiv:hep-ph/9602277.
[26] S. Catani, M.H. Seymour, Nucl. Phys. B 485 (1997) 291;
S. Catani, M.H. Seymour, Nucl. Phys. B 510 (1998) 503 (Erratum), arXiv:hep-ph/9605323.
[27] F. Cascioli, P. Maierhöfer, S. Pozzorini, Phys. Rev. Lett. 108 (2012) 111601, arXiv:1111.5206 [hep-ph].
[28] A. Denner, S. Dittmaier, L. Hofer, PoS LL2014 (2014) 071, arXiv:1407.0087 [hep-ph], 2014.
[29] A. Denner, S. Dittmaier, L. Hofer, arXiv:1604.06792 [hep-ph].
[30] A. Denner, S. Dittmaier, Nucl. Phys. B 658 (2003) 175, arXiv:hep-ph/0212259.
[31] A. Denner, S. Dittmaier, Nucl. Phys. B 734 (2006) 62, arXiv:hep-ph/0509141.
[32] A. Denner, S. Dittmaier, Nucl. Phys. B 844 (2011) 199, arXiv:1005.2076 [hep-ph].
[33] G. Ossola, C.G. Papadopoulos, R. Pittau, J. High Energy Phys. 0803 (2008) 042, arXiv:0711.3596 [hep-ph].
[34] A. van Hameren, Comput. Phys. Commun. 182 (2011) 2427, arXiv:1007.4716 [hep-ph].
[35] M. Grazzini, S. Kallweit, D. Rathlev, M. Wiesemann, J. High Energy Phys. 1508 (2015) 154, arXiv:1507.02565 [hep-ph].
[36] M. Wiesemann, arXiv:1602.03401 [hep-ph].
[37] S. Catani, L. Cieri, D. de Florian, G. Ferrera, M. Grazzini, Nucl. Phys. B 881 (2014) 414, arXiv:1311.1654 [hep-ph].
[38] S. Catani, L. Cieri, D. de Florian, G. Ferrera, M. Grazzini, Eur. Phys. J. C 72 (2012) 2195, arXiv:1209.0158 [hep-ph].
[39] T. Gehrmann, T. Lübbert, L.L. Yang, Phys. Rev. Lett. 109 (2012) 242003, arXiv:1209.0682 [hep-ph].
[40] T. Gehrmann, T. Lübbert, L.L. Yang, J. High Energy Phys. 1406 (2014) 155, arXiv:1403.6451 [hep-ph].
[41] T. Matsuura, S.C. van der Marck, W.L. van Neerven, Nucl. Phys. B 319 (1989) 570.
[42] M. Grazzini, S. Kallweit, D. Rathlev, A. Torre, Phys. Lett. B 731 (2014) 204, arXiv:1309.7000 [hep-ph].
[43] M. Grazzini, S. Kallweit, D. Rathlev, J. High Energy Phys. 1507 (2015) 085, arXiv:1504.01330 [hep-ph].
[44] R.D. Ball, et al., NNPDF Collaboration, J. High Energy Phys. 1504 (2015) 040, arXiv:1410.8849 [hep-ph].
[45] K.O. Mikaelian, M.A. Samuel, D. Sahdev, Phys. Rev. Lett. 43 (1979) 746.
[46] U. Baur, T. Han, J. Ohnemus, Phys. Rev. Lett. 72 (1994) 3941, arXiv:hep-ph/9403248.